ACS APPLIED MATERIALS & INTERFACES

Research Article

www.acsami.org

Determination of the Coalescence Temperature of Latexes by Environmental Scanning Electron Microscopy

Edurne Gonzalez,[†] Christopher Tollan,[‡] Andrey Chuvilin,[‡,§] Maria J. Barandiaran,[†] and Maria Paulis*[,†]

[†]POLYMAT, University of the Basque Country UPV/EHU, Joxe Mari Korta zentroa, Avda. Tolosa 72, 20018 Donostia-San Sebastián, Spain

[‡]CIC nanoGUNE Consolider, Avenida de Tolosa 76, 20018 Donostia-San Sebastián, Spain

[§]IKERBASQUE, Basque Foundation for Science, 48011, Bilbao, Spain

Supporting Information

ABSTRACT: A new methodology for quantitative characterization of the coalescence process of waterborne polymer dispersion (latex) particles by environmental scanning electron microscopy (ESEM) is proposed. The experimental setup has been developed to provide reproducible latex monolayer depositions, optimized contrast of the latex particles, and a reliable readout of the sample temperature. Quantification of the coalescence process under dry conditions has been performed by image processing based on evaluation of the image autocorrelation function. As a proof of concept the coalescence of two latexes with known and differing glass transition temperatures has been measured. It has been shown that a reproducibility of better than 1.5 °C can be obtained for the measurement of the coalescence temperature.

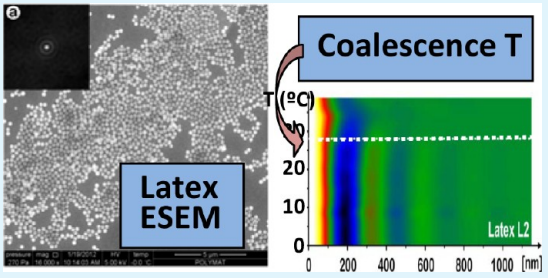

KEYWORDS: *acrylic copolymer latex, coalescence of soft colloidal particles, dry sintering, ESEM, autocorrelation function, quantification of coalescence temperature*

INTRODUCTION

Latexes are waterborne polymeric dispersions that are widely used as coatings, paints and adhesives, whose final purpose is the formation of a film. The transformation of the polymeric dispersion into a coherent polymer film is known as the film formation process and the evolution of this transformation strongly influences the final film properties. The film formation process can be divided into four main stages separated by three transitions[1−5] (Figure 1). Stage I corresponds to the initial wet state, the water dispersion of the polymer particles. Evaporation of water leads to stage II in which particles are in contact with each other, forming a close packed array with water filled interstices. During the transition to the next stage, interstitial water is lost and particles are deformed by van der Waals and capillary forces. Stage III is defined by a densely packed array in which deformed yet still discrete particles retain their identity. Stage IV is defined as a molecularly continuous film formed as a result of the diffusion of polymer chains across particle interfaces. This transition from III to IV can only occur above the glass transition temperature (T_g) of the polymer.

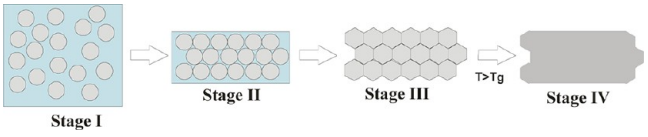

Figure 1. Film formation process.

The transition between stages III and IV is extremely important for the mechanical properties of the final film. The mechanical strength of a film is developed by the interdiffusion of chain ends and the formation of entanglements across the particle boundaries, therefore good cohesion of the film is not obtained until the polymers from neighboring particles have interdiffused across the particle boundaries.[6,7] As a consequence, reliable methods for studying this transition with accuracy are of great importance. Microscopic techniques based on TEM (transmission electron microscopy) and SEM (scanning electron microscopy) have been used to investigate the stages of film formation.[8−11] These techniques assume exposition of the samples to a high vacuum inside a microscope, and in many cases involve drastic steps for sample preparation, such as freeze-drying prior to analysis, which limits their use for the study of film formation dynamics. Other techniques have also been used to study the interdiffusion between particles, such as FRET (fluorescence resonance energy transfer)[2] and SANS (small angle neutron scattering),[12] or more recently synchrotron SAXS (small-angle X-ray scattering).[13−15] Never-

Received: May 31, 2012
Accepted: July 19, 2012
Published: July 19, 2012

theless, these techniques provide indirect measurements that require adequate interpretation of the data.

Environmental scanning electron microscopy (ESEM) is a technique that has shown great potential for the investigation of latexes, because it enables the study of microstructural changes occurring during film formation in the natural wet state of suspension. ESEM utilizes a differential pumping vacuum scheme, where a set of differentially pumped apertures separate a high vacuum section (column and the gun) from a low vacuum section (sample chamber). This allows the specimen to be observed under water vapor and other auxiliary gases such as nitrogen or nitrous oxide.[16] In modern instruments the sample chamber can be held at pressures up to 4000 Pa while the gun and the column remain at 1×10^{-5} to 1×10^{-7} Pa. Dehydration can be inhibited or even reversed by control of the sample temperature combined with a proper pump down procedure,[17] hence, wet samples can be imaged in their "natural state". Furthermore, this technique removes the need to cover nonconductive samples with a conducting layer.[18,19]

ESEM has been used by different groups to study the film formation of latexes.[18−24] Keddie et al[18,20] inserted a wet latex into the specimen chamber at 3 °C carrying out an evaporation inhibiting pump down without any significant loss of water from the latex sample. They were then able to observe the wet sample in its natural state. However, the real film formation process was done ex situ by drying the latexes at 20 °C outside of the ESEM and later inserting the latex-films into the microscope for observation after different drying times. In this way, the authors could observe differences in particle aggregation and coalescence for latexes with different T_g, after being dried for different lengths of time. Following this procedure Donald and co-workers[19,21−24] implemented the technique to visualize in situ aggregation of polymer particles in the presence of salts in the ESEM. In addition to the samples dried outside of the ESEM, they also followed in situ the dehydration of latex samples by increasing the sample temperature from 0 to 2 °C. Authors reported two problems with the suggested technique; on one hand they admitted the risk of beam damage by continuous imaging of the same area while the sample was dehydrating and on the other hand, they also considered that they were viewing only the top layer of the sample. This implies that unaccounted layers below could have influenced the process. Furthermore (though authors did not comment on this) for a multilayered latex stack it cannot be guaranteed that the particles on the top layer are at the same temperature as the ones just in contact with the holder. Therefore, to have representative and reproducible measurements, it is important to avoid prolonged exposure of the sample to the electron beam, and to perform the experiments with only a monolayer of particles.

In all of the works mentioned, the existence of the transition from non coalesced (stage III) to the coalesced particle state (stage IV) using ESEM was demonstrated, but in none of them were the ESEM data meant to provide quantitative characteristics of the process, in particular the transition temperature. This information is of key importance for understanding the influence and the mechanism of action of different formulations on the final properties of the films produced.

In fact, the coalescence would be the transition from the polymer particles that have been deformed to the interdiffusion of polymer chains between neighboring particles. This transition can be carried out in dry or wet conditions, depending on the rate of water evaporation. Therefore different mechanisms have been described in the literature to account for wet sintering,[18,25−27] sintering driven by capillary pressure[28−31] (under moisture conditions), and dry sintering.[32,33] As a first approach to observe the coalescence process we have chosen to carry out the study under dry conditions leaving a residual water pressure in the ESEM chamber in order to avoid working under more unrealistic vacuum conditions. The humidity in the chamber was controlled in a manner that ensured that water did not condense on the film.

The objective of this work is therefore to design a new working methodology for ESEM in order to observe in detail the coalescence process in dry conditions, and in that way be able to evaluate the temperature at which polymer particles start to coalesce by dry sintering. The method developed provides the means for unbiased temperature control of the process, minimizes beam damage artifacts, optimizes imaging conditions, and suggests an approach for extracting quantitative information from ESEM images. As a proof of concept, the methodology is applied to two test poly(methyl methacylate/butyl acrylate) (p-MMA/BA) latexes with different glass transition temperatures (T_g) (MMA/BA ratios: 50/50 and 55/45 wt %).

EXPERIMENTAL SECTION

Materials. Methyl metacrylate (MMA) and butyl acrylate (BA) monomers were used as received from Quimidroga (Spain) without further purification. Sodium laurylsulphate (SLS, Aldrich) was used as emulsifier and 4,4′-azobis (4-cyanovaleric acid) (V-501, Fluka) as initiator. Sodium hydroxide (NaOH, Panreac) was used to dissolve the initiator in water. Doubly deionized (DDI) water was used throughout the work.

Synthesis of MMA/BA Latexes by Emulsion Polymerization. MMA/BA latexes with different T_g values were synthesized by seeded semicontinuous emulsion polymerization. Initially, a seed with MMA/BA (50/50 wt %) at 10% solids content (S.C.) was prepared with SLS (1% weight based on monomers, wbm) and V-501 (1% wbm) in a 1000 mL glass jacketed reactor equipped with a reflux condenser, a N_2 inlet, a sampling device, a stainless steel modified anchor stirrer rotating at 250 rpm, and a cascade temperature control system (Camile TG, Biotage). The seed was used in the seeded semibatch emulsion copolymerization of MMA/BA (50/50 wt %) and MMA/BA (55/45 wt %) to produce L1 and L2 latexes respectively. The semibatch polymerizations were carried out as follows: The reactor was loaded with the desired amount of the polymer seed (20 wt %) and part of the water, and the temperature was increased to 70 °C. Upon achieving the required temperature, the initiator (V-501, 1% wbm), dissolved in water (6 wt %, adding a stoichiometric amount of NaOH), was introduced in a shot and the rest of the ingredients were fed in one stream containing the preemulsion of MMA and BA (62% S.C. and SLS 1% wbm) to achieve a final solids content of 40%. After the feeding period (4 h) the system was allowed to react in batch for one hour more. Conversion was measured by gravimetry. Particle sizes were determined by dynamic light scattering using a Malvern Nanosizer.

Minimum Film Formation Temperature (MFFT) and Glass Transition Temperature. The measurements of the MFFT of the latexes were carried out on a steel plate having a temperature gradient along it. The temperature at the point of the bar at which the film became optically clear and attained mechanical integrity was defined as its MFFT. The glass transition temperature of the polymers was determined by differential scanning calorimetry, DSC (Q2000, TA Instruments). The samples were dried, placed in an open pan, cooled to −50 °C and then heated to 200 at 10 °C/min.

Methodology of Latex Imaging in ESEM. Experiments were performed on a Quanta 250 FEG ESEM (FEI, Netherlands) equipped with Peltier cooling stage and GSE detector. The mechanism of image contrast formation by gaseous secondary electron detector (GSED) in

the ESEM under low pressure conditions is more complex as compared to topological contrast provided by SE detector or material contrast provided by BSE detector in high vacuum.[34] Substrates usually used to support colloids for imaging in high vacuum may not serve well at low pressure. In particular we have found that a flat silicon surface does not provide enough contrast for latex particles and thus requires application of a high electron dose in order to obtain a sufficient signal-to-noise ratio, which was found here to capable of significantly increasing the rate coalescence of the latex particles. As a follow-up a systematic search for the optimal substrate was carried out. The criteria for optimization included: maximum contrast of latex particles under low pressure conditions in order to minimize the electron dose, wettability for monolayer deposition and high thermal conductivity for correct temperature readout (Table 1). As has been

Table 1. Benefits and Limitations of Tested Substrates

substrate	benefits	limitations
silicon	flat surface	poor contrast, poor thermal conductivity, poorly wettable
mica	flat surface, wettable	poor thermal conductivity
glass (SiO_2)	high contrast, highly wettable	poor thermal conductivity
aluminum	high thermal conductivity	poor contrast, poorly wettable
gold	high thermal conductivity, wettable	poor contrast

demonstrated previously, insulating substrates like glass[35] and, as we found in this study, mica give better image contrast between organic materials and the substrate, which is consistent with the observations of other groups for similar low vacuum conditions and when using GSEDs.[36] There are thought to be various mechanisms by which image contrast is formed under these conditions[37−41] and they will not be discussed further in this study. However, despite the advantages obtained through use of an insulating substrate the thermal conductivity of a piece of glass or mica mounted on a SEM stub was considered to be unsuitable.

To combine the benefits and to avoid drawbacks we designed a special aluminum stub covered with a SiO_2 layer (see Figure 2). To

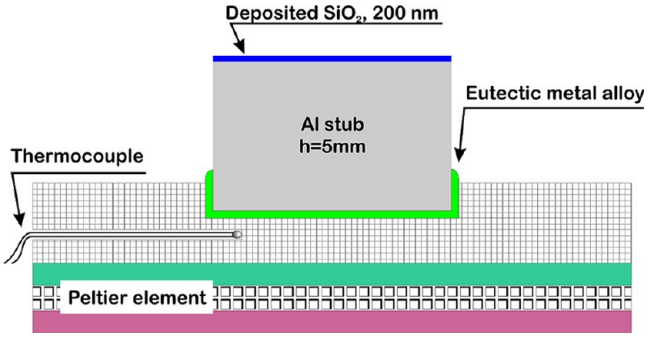

Figure 2. Scheme illustrating the experimental setup. A 5 mm height Al cylinder is mounted on a standard Peltier stage by thermoconducting grease or metal alloy. The surface of the cylinder is mirror polished and covered by 200 nm of SiO_2.

ensure a minimal temperature gradient between the thermocouple and the deposited sample, the height of a standard cylindrical (⌀ 9.5 mm) aluminum stub was decreased to 5 mm and the upper face was polished to a mirror finish. The final polished surface was obtained using colloidal silica. On this polished surface a layer of SiO_2 (200 nm) was deposited in order to provide optimal imaging contrast. Thus prepared stub was mounted onto a Peltier cooling stage using a eutectic metal alloy (Fusible Alloy 47, INNOVATOR Sp. z o.o.) with a low melting temperature (47 °C) in order to ensure a good heat conductance.

To obtain monolayer coverage of polymer particles on the stub surface a fraction of the latex was diluted to 0.1% of solids content. A drop of the diluted latex was placed onto the stub at a stage temperature of 0 °C and a controlled pump down of the sample chamber was performed until a pressure of 270 Pa was obtained. Water vapor was used to create pressure inside the ESEM chamber and thus the startup humidity in the proximity of the sample was 42%. Once initial conditions were set, the pressure was maintained constant and the temperature was increased gradually in a controlled way as illustrated in Figure 3. The temperature increment in each step was

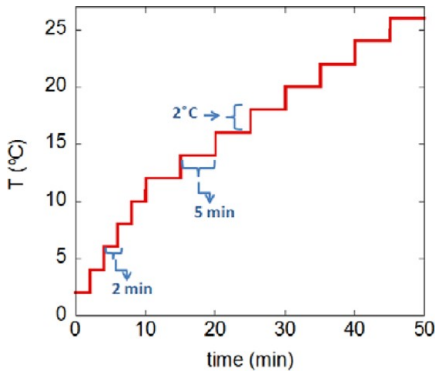

Figure 3. Temperature ramp used in the ESEM experiment.

2 °C (heating rate: 20 °C/min). The T_g values for the polymers were above 10 °C in both cases (no coalescence was expected until this temperature), therefore from 0 to 10 °C the sample was left only for 2 min at each temperature. However, from 10 °C onward samples were left for 5 min at each temperature in order to give them enough time to reach the thermal equilibrium.

Engqvist et al. showed that the deformation at room temperature of styrene/acrylic particles with a T_g similar to the ones of the copolymers used in this work, over a SiO_2 substrate was almost negligible after 48 h.[42] Therefore, and taking into account that our whole experiment does not last more than 2 h, it can be assumed that the influence of the substrate used in this work (SiO_2) on the coalescence process of a monolayer of particles with the glass transition temperatures (T_g) presented by the copolymers used is negligible.

To minimize the influence of beam damage, check the reproducibility, and provide a good statistics for image processing, we took four to five images at different locations on the sample for each temperature step. Images taken at an unirradiated location ensured that the sample was undamaged at every given temperature. Then, immediately after acquisition, the irradiation was stopped (the beam was blanked) until the next temperature was reached. The same procedure was repeated for each temperature. The flat surface of the stub and almost continuous monolayer coverage gave the possibility to move "blind" to any arbitrary site on the sample without loss of focus. Following this procedure it was possible to track the temperature at which particles started to coalesce for each of the latex samples.

The imaging conditions of the microscope were as follows: accelerating voltage 5 kV, spot size 3, working distance 6.8 mm, GSE detector (500 μm).

Image Processing and Quantification. In the current work, we were aiming to establishing a quantitative criterion derived from ESEM images that would reflect the coalescence of latex particles. In an ideal case this criteria should respond to the coalescence only and should be robust in respect to image parameters such as intensity and contrast of the image, amount of latex particles on the image, presence of other features, etc. We have found that an autocorrelation function[43] responds very well to the coalescence process. Oscillations of the autocorrelation function (Figure 4a inset and Figure 4b) reflect a near order in latex packing, thus the first maximum corresponds to the

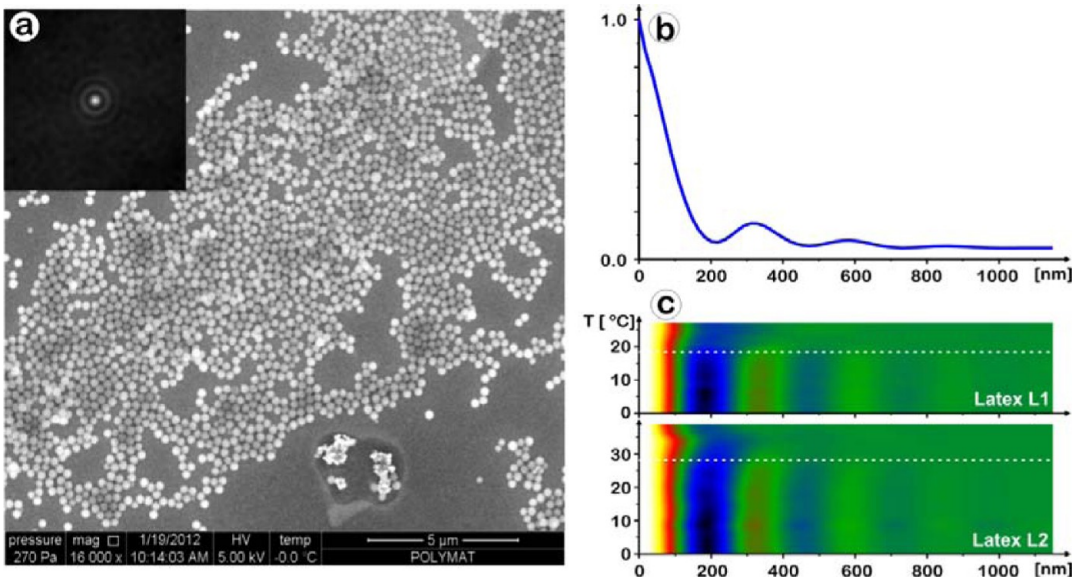

Figure 4. (a) Representative ESEM image of sample L2, an insert shows corresponding 2D autocorrelation function; (b) rotationally averaged autocorrelation function; (c) 2D plots of autocorrelation function vs temperature for test samples; approximate temperature of transition from separate particles to flat surface is seen as vanishing of oscillations and is marked by dashed lines.

distance between the centers of the spheres. The 2D color coded plot in Figure 4c represents the dependence of the azimuthally averaged autocorrelation function of the images of the latexes as a function of temperature. The transition from separate latex spheres to a flat film is reflected by the vanishing oscillations. This transition can be clearly seen by visual inspection.

Physically, coalescence is visualized as a decrease of sharpness (smearing) of the interface between adjacent particles. Mathematically this may be expressed as a decrease of curvature (a second derivative) of the intensity profile plotted on the image from one particle to another. As an average criterion over the whole image a decrease of the second derivative of the autocorrelation function may be used. Thus the difference between the minimum and maximum of the second derivative may be used as an estimate of the homogeneity (lack of interfaces between polymer particles) of the film.

As a presumption for a robust measurement, an image should contain a substantial area covered by closely packed latex particles, which was relatively easy to achieve experimentally. Far order in the particle arrangement is not required; nevertheless, particles should contact each other, providing many interfaces for good statistics. To improve the estimate even further, additional filtering is done on the image, which suppresses the areas with a poor featureless autocorrelation, thus eliminating the background noise caused by stand alone particles and dust.

The work flow of image processing is then as follows:

(1) background subtraction in order to enhance higher spatial frequencies and to eliminate broad features in the autocorrelation function;
(2) filtering away areas of the image without adjacent particles;
(3) calculation of autocorrelation;
(4) calculation of radial profile of the autocorrelation function;
(5) calculation of the second derivative of the radial profile;
(6) detection of maxima and minima of the second derivative.

METHODOLOGY TEST ON REFERENCE SAMPLES

Two different latexes of MMA/BA (50/50 wt % (L1) and 55/45 wt % (L2)) at 40% S.C. using SLS as an emulsifier were synthesized by seeded semibatch emulsion polymerization. The properties of the latexes are compared in Table 2. Both latexes presented very similar particle sizes. Regarding the film properties, it can be observed that as expected, the T_g and the MFFT values increased as the MMA weight ratio used in the formulation increased.

Table 2. Properties of the Different Latexes Used in This Study

name	MMA/BA (wt %)	emulsifier	S.C. (%)	dp (nm)	MFFT (°C)	T_g (°C)
L1	50/50	SLS	41	276	10	18
L2	55/45	SLS	40	272	17	27

The samples for ESEM were prepared as described above. In a series of preliminary test experiments the samples were placed into the microscope chamber at a pressure (640 Pa) exceeding the dew point of water at 0 °C and the drying process was observed in situ (see the Supporting Information) in a similar manner to previous reports.[18−24] After drying at 270 Pa the latex monolayer was found to be in the same state as the samples predried in air, which ensured that no artifacts were introduced by the proposed ESEM sample preparation procedure. Experiments were repeated within a time frame of several months in order to check reproducibility.

After the initial temperature and pressure were set, the latex was dried and while the water vapor pressure in the microscope chamber was maintained at a constant value (270 Pa), the temperature was ramped up as described above (Figure 3). Figures 5 and 6 show images obtained during the temperature ramp for latexes L1 and L2, respectively.

As can be seen, the particles in L1 retained their initial shape up to 16 °C. Coalescence started at 18 °C and was almost complete at 22 °C. There is a clear difference for the case of L2, where particles retained their identity until 24 °C and started to coalesce at 26 °C. From 26 to 28 °C, the coalescence was partial and at 30 °C it can be considered that most of the particles had coalesced. In Figure 6f, it can be seen that at 32 °C the film was fully formed.

Application of the image processing described above gives an exact value for the transition temperature as well as characterizing the temperature range of the transition. Figure 7a represents plots of the difference between the maximum and

dx.doi.org/10.1021/am300971v | ACS Appl. Mater. Interfaces 2012, 4, 4276−4282

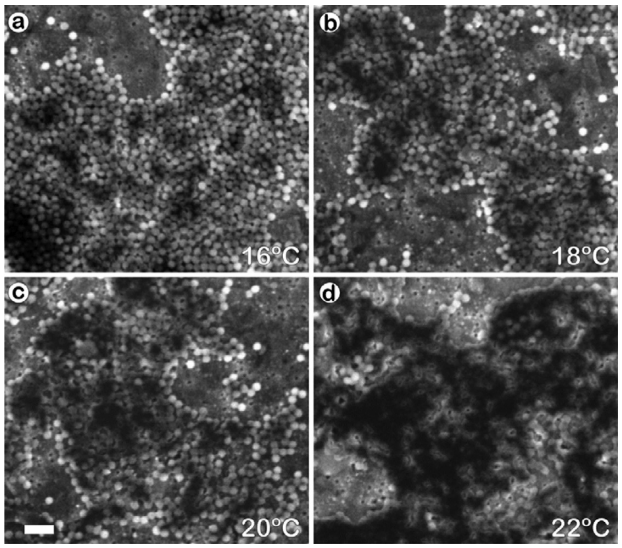

Figure 5. ESEM images for latex L1 obtained at different temperatures, in all the cases the pressure was 270 Pa: (a) 16, (b) 18, (c) 20, and (d) 22 °C. The length of the scale bar is 1 μm.

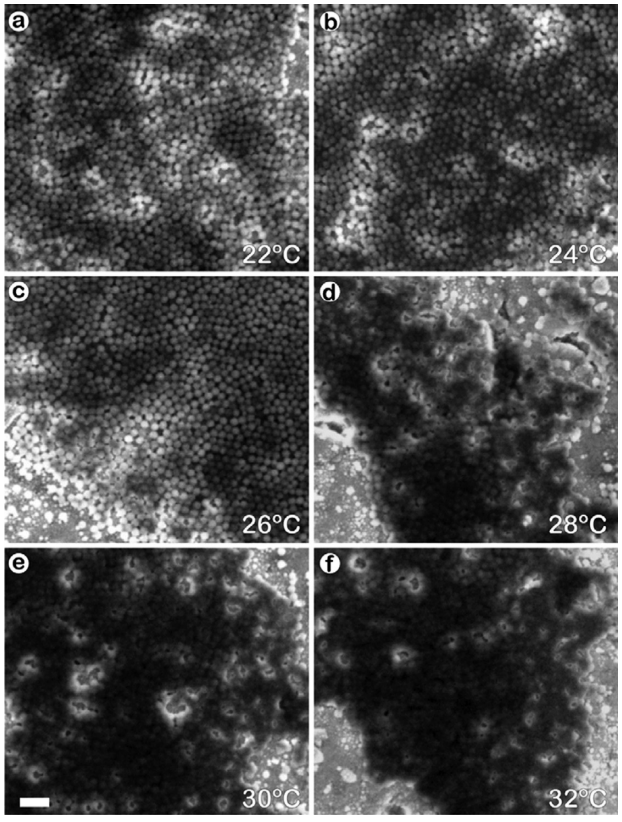

Figure 6. ESEM images for latex L2 obtained at different temperatures, in all cases the pressure was 270 Pa: (a) 22, (b) 24, (c) 26, (d) 28, (e) 30, and (f) 32 °C. The length of the scale bar is 1 μm.

minimum values of the second derivative of the autocorrelation function (normalized to 1 for every sample) as a function of temperature. The symbols mark the experimental data points for latexes L1 and L2, and L1 Rep and L2 Rep for a repeated set of experiments. In all cases data shows a plateau at low temperatures where no changes are observed in the separate particles, and a plateau at high temperatures where a

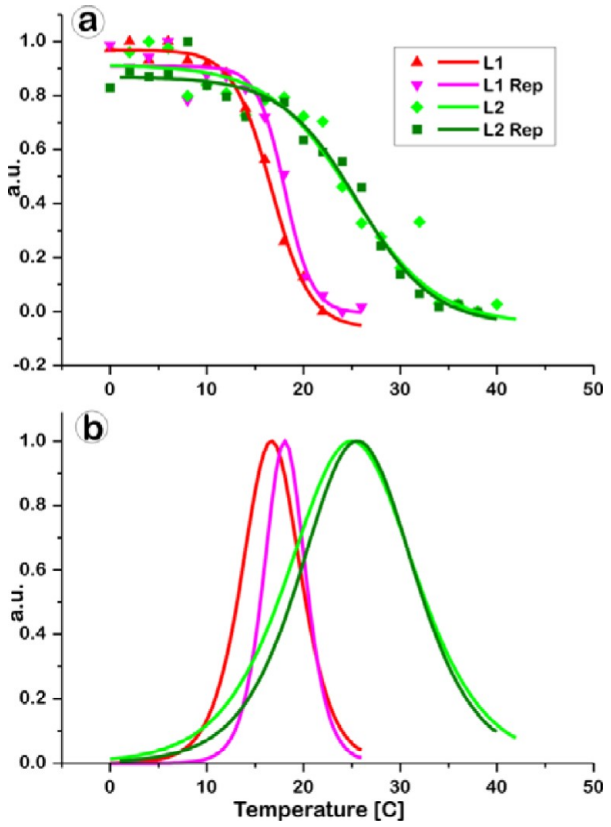

Figure 7. (a) Plot of the normalized value of the estimator defined in the text against temperature for two sets of the two test samples (L1 and L2); experimental points are fitted by Boltzmann function; (b) derivatives of Boltzmann functions at (a); maxima of peaks defines the transition temperature, while the breadth corresponds to the transition interval.

continuous film has formed. A gradual decrease of the value of the estimator at intermediate temperatures reflects the increase of the flatness (lack of boundaries) of the film surface. The Boltzmann function gives a good fit for experimental points and corresponding curves are overlaid on the graph. Figure 7b represents the derivatives of fitted Boltzmann functions to highlight the position and breadth of the transitions.

The transition temperature estimated as a temperature of a maximum transition velocity (maximum of the derivative) is 16.7 and 18.0 °C in two experiments for latex L1, and 25.0 and 25.5 °C for latex L2 correspondingly. The variation between the coalescence temperatures obtained in the two separate experimental sets is below 1.5 °C in both cases and this value defines the precision of the proposed method. In both cases there is a remarkable agreement between ESEM measurements and glass transition temperature measured by DSC. The breadth of the transition is also observed by DSC and can be attributed to the width of the molecular weight distribution. A slight shift of ESEM measured values to lower temperatures may be attributed to the fact that the maximum coalescence velocity is reached at the temperature just below T_g and the ESEM method appears to be able to get a snapshot of this process. The dynamics of coalescence observed and quantified in ESEM can be correlated to give a general understanding of the phenomena observed on the macroscopic scale.

It should be pointed out that this is the first time in which the coalescence temperature of latex particles has been

quantified so precisely by ESEM. Previous works on the study of film formation by ESEM had been centered on the packing of polymer particles during film formation[19,21] or on the effect of the addition of non film forming particles.[20] Furthermore, in most cases, the formation of the film has happened outside the microscope or instantaneously by an increase of the chamber temperature by less than 5 °C.[18−23] The procedure presented in this work therefore presents a new approach, as it aims to quantify the exact temperature at which the coalescence between particles occurs in a direct way, differing from the indirect methods typically used, such as SANS or FRET.[5]

CONCLUSIONS

In this work, we have developed a methodology to quantify the temperature at which the coalescence between polymer particles in latexes occurs during film formation by ESEM. To validate our method, we synthesized two different latexes by seeded semibatch emulsion copolymerization; PMMA-co-PBA 50/50 wt % (T_g = 18 °C) and PMMA-co-PBA 55/45 wt % (T_g = 27 °C). The deposition of the latex on an appropriate stub (aluminum coated with SiO_2), especially designed to increase image contrast and thermal conductivity, was optimized in order to obtain a monolayer coverage. A preset sequence of heating and observations was established in order to acquire images of the latex state at accurate temperatures and to reduce the damage of the sample by the beam. To be able to quantify the coalescence process, we used the autocorrelation function of the images. This way, the coalescence temperature was determined with a precision better than 1.5 °C, observed after the reproduction of the coalescence experiment for the same latex sample. For both latexes, the coalescence temperature under dry conditions was found to be correlated to their glass transition temperature.

In conclusion, the methodology proposed in the present work offers the possibility to quantify the coalescence temperature of polymer particles in latexes. Even if in this case copolymers with different T_g have been used, the method offers the possibility to study the effect of different agents that may change the apparent T_g of the polymer which in turn affects the coalescence between particles. Thus, the effect of coalescing agents or of core−shell structures that favor film formation could be quantified from the coalescence temperature point of view. Furthermore, the possibilities regarding the study of the effect of different polymer particle surface stabilizers on the film formation properties has a potentially broad range. It cannot be forgotten that the coalescence process is highly important for obtaining glossy and non permeable films.

This method will be also of use to others studying colloidal systems, such as in nanomaterials, adhesives, foods, biomaterials, etc. By making the analysis quantitative and reliable, the work has the potential to increase the use of ESEM in the analysis of colloidal materials.

ASSOCIATED CONTENT

Supporting Information

In situ drying process observed in preliminary test experiments, where the samples were placed into the microscope chamber at a pressure (640 Pa) exceeding the dew point of water at 0 °C. This material is available free of charge via the Internet at http://pubs.acs.org.

AUTHOR INFORMATION

Corresponding Author

*E-mail: maria.paulis@ehu.es.

Notes

The authors declare no competing financial interest.

ACKNOWLEDGMENTS

The financial support by the Industrial Liaison Program of POLYMAT and FEI company (Netherlans) in the form of a collaboration project is gratefully acknowledged. The financial support by UPV/EHU through UFI11/56 is also gratefully acknowledged.

REFERENCES

(1) Boczar, E. M.; Dionne, B. C.; Fu, Z.; Kirk, A. B.; Lesko, P. M.; Koller, A. D. *Macromolecules* **1993**, *26*, 5772−5781.
(2) Wang, Y.; Winnik, M. A. *J. Phys. Chem.* **1993**, *97*, 2507−2515.
(3) Peckan, O. *Trends Polym. Sci.* **1994**, *2*, 236−243.
(4) Keddie, J. L. *Mat. Sci. Eng.* **1997**, *21*, 101−170.
(5) Keddie, J. L.; Routh, A. F., *Fundamentals of Latex Film Formation*; Springer: New York, 2010.
(6) Yoo, J. N.; Sperling, L. H.; Glinka, C. J.; Klein, A. *Macromolecules* **1990**, *23*, 3962−3967.
(7) Daniels, E. S.; Klein, A. *Prog. Org. Coat.* **1991**, *19*, 359−378.
(8) Roulstone, B. J.; Wilkinson, M. C.; Hearn, J.; Wilson, A. J. *Polym. Int.* **1991**, *24*, 87−94.
(9) Wang, Y.; Kats, A.; Juhue, D.; Winnik, M. A.; Shivers, R. R.; Dinsdale, C. J. *Langmuir* **1992**, *8*, 1435−1442.
(10) Eckersley, S. T.; Rudin, A. *J. Appl. Polym. Sci.* **1993**, *48*, 1369−1381.
(11) Joanicot, M.; Wong, K.; Richard, J.; Maquet, J.; Cabane, B. *Macromolecules* **1993**, *26*, 3168−3175.
(12) Kim, S. D.; Klein, A.; Sperling, L. H.; Boczar, E. M.; Bauer, B. J. *Macromolecules* **2000**, *33*, 8334−8343.
(13) Hu, S.; Rieger, J.; Roth, S. V.; Gehrke, R.; Leyrer, R. J.; Men, Y. *Langmuir* **2009**, *25*, 4230−4234.
(14) Hu, S.; Rieger, J.; Yi, Z.; Zhang, J.; Chen, X.; Roth, S. V.; Gehrke, R.; Men, Y. *Langmuir* **2010**, *26*, 13216−13220.
(15) Chen, X.; Fisher, S.; Yi, Z.; Boyko, V.; Terrenoire, A.; Reinhold, F.; Rieger, J; Li, X; Men, Y. *Langmuir* **2011**, *27*, 8458−8463.
(16) Meredith, P.; Donald, A. M. *J. Microscopy* **1996**, *181*, 23−35.
(17) Cameron, R. E.; Donald, A. *J. Microscopy* **1994**, *173*, 227−237.
(18) Keddie, J. L.; Meredith, P.; Jones, R. A. L.; Donald, A. M. *Macromolecules* **1995**, *28*, 2673−2682.
(19) Donald, A. M.; He, C.; Royall, P.; Sferrazza, M.; Stelmashenko, N. A.; Thiel, B. L. *Colloids Surf., A* **2000**, *174*, 37−53.
(20) Keddie, J. L.; Meredith, P.; Jones, R. A. L.; Donald, A. M. *Langmuir* **1996**, *12*, 3793−3801.
(21) Dragnevski, K. I.; Donald, A. M. *Colloids Surf., A* **2008**, *317*, 551−556.
(22) Dragnevski, K. I.; Donald, A. M. *Prog. Org. Coat.* **2008**, *61*, 63−67.
(23) Dragnevski, K.; Donald, A.; Taylor, P.; Murray, M.; Davies, S.; Bone, E. *Macrom. Symp.* **2009**, *281*, 119−125.
(24) Dragnevski, K. I.; Donald, A. M.; Taylor, P.; Murray, M. W.; Bone, E. L.; Davies, S. J. *Prog. Org. Coat.* **2009**, *65*, 19−24.
(25) Vanderhoff, J. W.; Tarkowski, H. L.; Jenkins, M. C.; Bradford, E. B. *J. Macromol. Chem.* **1996**, *1* (2), 361−397.
(26) Sheetz, D. P. *J. Appl. Polym. Sci.* **1965**, *9*, 3759−3773.
(27) Dobler, F.; Pith, T.; Holl, Y.; Lambla, M. *J. Appl. Polym. Sci.* **1992**, *44*, 1075−1086.
(28) Brown, G. L. *J. Polym. Sci.* **1956**, *22*, 423−434.
(29) Mason, G. *Br. Polym. J.* **1973**, *5*, 101−108.
(30) Eckersley, S. T.; Rudin, A. *J. Appl. Polym. Sci.* **1994**, *53*, 1139−1147.
(31) Lin, F.; Meier, D. J. *Langmuir* **1995**, *11*, 2726−2733.

(32) Dillon, R. E.; Mattheson, L. A.; Bradford, E. B. *J. Colloid Sci.* **1951**, *6*, 108−117.
(33) Sperry, P. R.; Snyder, B. S.; O'Dowd, M. L.; Lesko, P. M. *Langmuir* **1994**, *10*, 2619−2628.
(34) Baroni, T. C.; Griffin, B. J.; Browne, J. R.; Lincoln, F. J. *Microsc. Microanal.* **2000**, *6*, 49−58.
(35) Stokes, D. J.; Rea, S. M.; Best, S. M.; Bonfield, W. *Scanning* **2003**, *25*, 181−184.
(36) Toth, M.; Thiel, B. L.; Donald, A. M. *Ultramicroscopy* **2003**, *94*, 71−87.
(37) Toth, M.; Phillips, M. R.; Thiel, B. L.; Donald, A. M. *J. Appl. Phys.* **2002**, *91*, 4479.
(38) Toth, M.; Kucheyev, S. O.; Williams, J. S.; Jagadish, C.; Phillips, M. R.; Li, G. *Appl. Phys. Lett.* **2000**, *77*, 1342.
(39) Toth, M.; Phillips, M. R. *Scanning* **2000**, *22*, 313.
(40) Craven, J. P.; Baker, F. S.; Thiel, B. L.; Donald, A. M. *J. Microsc.* **2002**, *205*, 96.
(41) Toth, M.; Thiel, B. L.; Donald, A. M. *J. Microsc.* **2002**, *205*, 86.
(42) Engqvist, C.; Forsberg, S.; Norgren, M.; Edlund, H.; Andreasson, B.; Karlsson, O. *Colloids Surf., A* **2007**, *302*, 197−203.
(43) Russ, J. C. *The Image Processing Handbook*, 6th ed.; CRC Press: Boca Raton, FL, 2011.